AD-A097 390 WASHINGTON STATE UNIV PULLMAN DEPT OF PHYSICS F/G 11/4
THE EMISSION OF ELECTRONS AND POSITIVE IONS FROM FRACTURE OF MA--ETC(U)
APR 81 J T DICKINSON, E E DONALDSON, M K PARK N00014-80-C-0213
UNCLASSIFIED TR-1 NL

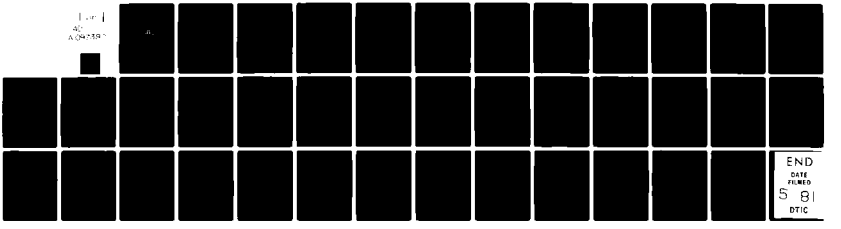

END
DATE FILMED
5 81
DTIC

(14) TR-1

SECURITY CLASSIFICATION OF THIS PAGE (When Data Entered)

REPORT DOCUMENTATION PAGE		READ INSTRUCTIONS BEFORE COMPLETING FORM
1. REPORT NUMBER: Technical Report No. 1	2. GOVT ACCESSION NO.: AD-A097390	3. RECIPIENT'S CATALOG NUMBER
4. TITLE (and Subtitle): The Emission of Electrons and Positive Ions from Fracture of Materials		5. TYPE OF REPORT & PERIOD COVERED: Technical Report
		6. PERFORMING ORG. REPORT NUMBER
7. AUTHOR(s): J. T. Dickinson, E. E. Donaldson and M. K. Park		8. CONTRACT OR GRANT NUMBER(s): N00014-80-C-0213
9. PERFORMING ORGANIZATION NAME AND ADDRESS: Physics Department, Washington State University, Pullman, WA 99164		10. PROGRAM ELEMENT, PROJECT, TASK AREA & WORK UNIT NUMBERS: NR 092-558
11. CONTROLLING OFFICE NAME AND ADDRESS: Office of Naval Research, Power Program, Arlington, VA 22217		12. REPORT DATE: April 1, 1981 13. NUMBER OF PAGES: 32
14. MONITORING AGENCY NAME & ADDRESS (if different from Controlling Office)		15. SECURITY CLASS. (of this report): Unclassified
		15a. DECLASSIFICATION/DOWNGRADING SCHEDULE

16. DISTRIBUTION STATEMENT (of this Report)

Approved for public release; distribution unlimited

17. DISTRIBUTION STATEMENT (of the abstract entered in Block 20, if different from Report)

18. SUPPLEMENTARY NOTES

Submitted to Journal of Materials Science

19. KEY WORDS (Continue on reverse side if necessary and identify by block number)

fracture, delamination, crack propagation, fracture surfaces, interfacial failure, exo-emission, electron emission, tribo-stimulated exo-emission, chemi-emission, surface charging, fracture of: crystalline materials, insulators, polymers, fibers, filaments, glass, mica, carbon, rubber, fiber-reinforced epoxy, glass-filled polybutadiene.

20. ABSTRACT (Continue on reverse side if necessary and identify by block number)

The emission of electrons and positive ions from materials undergoing fracture is investigated. We present a survey of charged particle emission from a number of materials including crystalline insulators, glass, graphite, polymers, and composites. Particular attention is given to fiber-reinforced epoxy systems which yield unique forms of charge emission. Energy distributions of the emitted particles are given for E-glass/epoxy strands, polybutadiene filled with glass beads, and mica. Evidence is presented that interfacial failure and charge separation play important roles in the observed emission.

DD FORM 1 JAN 73 1473 EDITION OF 1 NOV 65 IS OBSOLETE S/N 0102 LF 014-6601

SECURITY CLASSIFICATION OF THIS PAGE

81 4 6 04

AD A097390

DTIC FILE COPY

DTIC ELECTE APR 6 1981 C

THE EMISSION OF ELECTRONS AND POSITIVE IONS FROM FRACTURE OF MATERIALS

by

J. T. Dickinson, E. E. Donaldson, and M. K. Park

Department of Physics
Washington State University
Pullman, WA 99164

ABSTRACT

The emission of electrons and positive ions from materials undergoing fracture is investigated. We present a survey of charged particle emission from a number of materials including crystalline insulators, glass, graphite, polymers, and composites. Particular attention is given to fiber-reinforced epoxy systems which yield unique forms of charge emission. Energy distributions of the emitted particles are given for E-glass/epoxy strands, polybutadiene filled with glass beads, and mica. Evidence is presented that interfacial failure and charge separation play important roles in the observed emission.

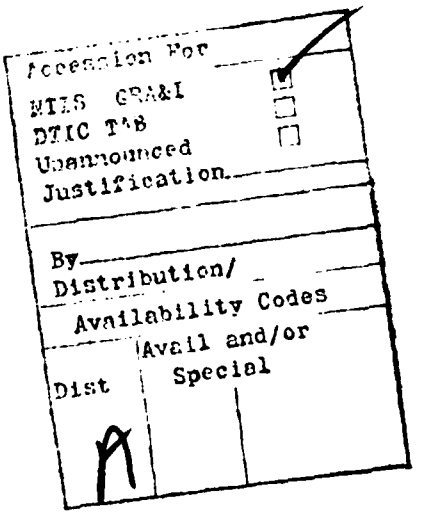

INTRODUCTION

During and following fracture of solids, the emission of charged particles,[1-6] neutral particles,[7] and photons[3,8,9] have been observed. Studies of electron emission (EE) during the tensile elongation of oxide-coated aluminum, sometimes referred to as tribo-stimulated exoemission, have shown that fracture of the oxide coating is the initial cause of the ejected electrons.[4-6] Similarly, positive ion emission (PIE) neutral emission[6] and photon emission[3] have been observed on the same oxide-aluminum system, and were shown to be due to oxide fracture. (Photon emission is most frequently referred to as tribo-luminescence.) These various types of emission share a number of common features, suggesting common mechanisms in their production. We refer to all forms of such emission accompanying fracture as "fracto-emission" (FE).

Basically, FE is caused by the high concentration of energy deposited into a small volume of material during crack propagation. For a short time period (microseconds or less) this can result in the following:

(1) production of highly localized heat;

(2) creation of excitations and defects in the material;

(3) production of dangling bonds and trapped electrons on or near the freshly created crack wall surface;

(4) the emission of excited and reactive species (ions and neutrals) into the gas phase;

(5) separation of charges on the crack walls with accompanying intense electric fields for many insulating materials; and

(6) production of acoustic waves.

In principle, all of the above consequences of crack growth could contribute to FE from the material. For large band gap insulators it is doubtful that

the peak localized temperatures reached are sufficient to elevate the valence band electrons thermionically into the vacuum. However, the temperature maxima reached might be quite adequate to excite and release electrons from surface traps. Likewise, thermal stimulation of the defects produced during fracture can lead to a number of de-excitations and recombinations which produce electron, ion, and neutral particle emission as well as photons.[10,11]

The interaction of excited and reactive species at a surface can readily produce electrons, free ions, and photons via Auger de-excitation,[12] stimulated desorption,[13,14] chemi-emission,[15] and chemiluminescence,[16] particularly on a highly reactive surface such as the freshly created crack wall. The significant differences between a clean crystal surface and a freshly created cleavage surface on silica and quartz has been investigated by Hochtrasser and Antonni.[17] They demonstrated that a high density of dangling bonds as well as the increase in chemical reactivity occurs upon fracture. Thus, it is reasonable to assume that freshly fractured surfaces of all materials would have considerable reactivity. In the case of polymers, for example, electron spin resonance investigations show that fractured polymers have high radical concentrations particularly in the case of highly crystalline oriented fibers.[18] It was suggested that cross-linkage enhances the type of fracture (presumably molecular fracture) that produces free radicals.

Clearly, fractured surfaces are potentially very reactive and could be expected to produce emission. For example, a reactive species, perhaps from the fractured material itself or from the background gases, can react with a site of high reactivity on the surface with sufficient energy release (Kasemo[15,16] suggests via an excited, adsorbate-induced hole state) during de-excitation to yield electrons or photons.

The separation of charges that occurs during fracture of ionic crystals[19] is known to produce electric field intensities that can exceed 15,000 V/cm. Such fields can contribute to electron emission by providing accelerating fields; e.g. electrons having energies as great as 120 keV have been observed coming from alkali halides.[20] Ions with kinetic energies of a few hundred eV have been observed coming from granite specimens.[21] During thermally stimulated exoemission, several other substances have exhibited electron emission with energies in the range from 5 eV to 10 keV.[22,23]

Other phenomena associated with the high temperatures produced at the crack tip involve thermal decomposition, diffusion of impurities, and the desorption of decomposition and diffusion species into the gas phase. For example, we have found the neutral emission from thin anodized coatings on Al to be very intense and intimately related to oxide cracking.[7] The species observed (e.g. O_2, H_2O, and CO_2) and intensities were dependent on the type of anodizing electrolyte used (H_3PO_4 and ammonium tartrate) and the oxide thickness. There was strong evidence that thermal decomposition and diffusion were involved in the release of the gases. Fox and Soria-Ruiz[24] detected gases released during fracture from a number of inorganic materials. They observed intense bursts of products due to both endothermic and exothermic reactions. Urakaev et al[25] saw volatile products and evidence of highly excited ions and radicals from mechanical fracture of inorganic crystals. Regel et al[26] saw intense neutral emission during fracture of PMMA, observing several mass peaks. The mass spectra observed were very similar to thermal decomposition products. Andrews[18] points out that the observed material evolving from the fractured polymers may be low molecular weight species already present in the specimen which are released by stress-assisted diffusion rather than thermally-activated decomposition.

Finally we mention that the stress wave created as the crack-tip moves through the material could in principle contribute to FE. Asay[27] has examined shock induced vaporization and has seen significant amounts of mass ejected from surfaces accelerated by strong shock waves. Hayes[28] has seen electrical effects on shocked materials that suggest that charged particles might be leaving the surface. Although the shock intensity is significantly higher in these studies than created by fast crack growth, the stress wave might contribute to part of the emission observed during fracture.

In this paper present recent results on FE, in particular charged particle emission, from crack propagation in a wide variety of materials. We compare the properties of this emission from homogeneous materials with emission from composite materials. In all the materials tested, some form of FE was observed and was most intense in materials where interfacial failure could occur. The types of materials tested were crystalline insulators, glasses, polymers (including elastomers), and composites.

EXPERIMENT

In almost all cases to be described here, catastrophic fracture was carried out on samples of two geometries:

(a) a rectangular parallelepiped broken in a three point bending mode for very brittle materials, and

(b) tensile specimens, notched in the center.

Loading was relatively slow, typically at strain rates of 1% per sec until rupture. Typical dimensions were such that the fractured surfaces had a cross-section from 5 to 20 mm^2. In addition we also fractured a number of bare filaments, typically 10μm in diameter, of materials such as glass, graphite, and Kevlar. These were mounted so that single filaments could be broken sequentially.

Also, epoxy-strands of some of these materials were fractured, the strands being provided to us by Lawrence Livermore Laboratory. Each strand contained approximately 250 filaments. The filament diameters were 20μm for E-glass and 10μm for S-glass and graphite. The filaments were untreated and the epoxy was Dow DER 332.

Most experiments were carried out in a vacuum chamber pumped by a diffusion pump with a liquid nitrogen cold trap. The background pressure was 2-4 x 10^{-6} Torr and the residual gases consisted primarily of CO, H_2O, and CO_2.

Some samples were also tested in an ion pumped vacuum system at a pressure of 10^{-8} Torr to determine the influence of the background gases. As discussed later, no differences between the two environments were observed.

Charged particles were detected with a channel electron multiplier (CEM), a Galileo Electro-Optics Model 4039, positioned 2 cm from the sample.

The front of the CEM was biased at +300 volts for efficient detection of electrons and at -2400 volts for detection of positive ions.[29] For a few materials, electric and magnetic fields were introduced with grids and permanent magnets to test for the presence and energy of charged particle emission. The pulse output (10ns pulse width) of the CEM was amplified and fed to a 100 mHz discriminator which drove a counter, a count rate meter, and a multichannel analyzer (MCA) allowing counts vs time to be recorded. The time domains used were usually two extremes: slow (0.8 sec/channel) or fast (1-1000 μs/channel). For our survey of materials, the slow time domain was used for determining the existence of FE and relative intensities. For a few materials, the fast time domain was used to measure the decay of the emission following fracture. The time of fracture was determined either with a stress transducer on the pulling mechanism or with an acoustic emission transducer attached to the sample mount.

For all materials studied, we looked for electrons, and in some cases, positive ions. The ion species involved in the PIE have not yet been determined.

RESULTS

A. Survey of Materials

Tables I and II present a summary of the observed electron and positive ion emission. It should be noted that we have not tested comprehensively for PIE. In all cases tested, EE and/or PIE have been observed, i.e., we have not as yet found a material which does not emit.

In each case, the emission intensity vs time curves have a common characteristic: highest intensity at or very near fracture, followed by a decay of emission. In some materials, the decay is with time constants on the order of μs or ms. Figure 1a shows an example of this behavior for the EE accompanying the fracture of polystyrene. Other materials exhibit emission that decays much slower, on the order of several seconds; this is shown for boron nitride in Fig. 1b. (Note the time scales.) In Tables I and II, the emission intensity is that measured over approximately one lifetime of the slowest decay constant. In cases where we have not measured the short decay times, we denote upper limits.

For a few materials, we applied a magnetic field of 0.01 Tesla to verify that the EE observed was indeed due to electrons rather than negative ions, excited neutrals, or short wavelength photons. This field was sufficiently low that negative ions with at least 1 eV energy would reach the electron multiplier, but strong enough that electrons because of their lower mass, would require over 300 eV to be detected. In the case of polystyrene, this field stopped all of the EE and approximately 80% of the EE from an E-glass-epoxy strand. The latter result suggested either high energy electrons are

created and/or a detectable component uninfluenced by a weak magnetic field is produced. The CEM is senstive to UV photons with wavelengths below 1200 Å and to metastable molecules with excitation energies above approximately 6eV.[29] It appears, however, that the EE observed is principally due to electrons.

For a few materials, the samples were plated with 30-50 nm of gold to provide a conducting surface at ground potential. This layer dissipated static surface charges due to handling of the sample. This surface charge caused large fluctuations in the observed EE, but had little effect on the PIE. This suggested that the surface charge was deflecting the electrons away from the +300 volt front cone of the CEM, but had little effect on the PIE due to the -2400 volts applied to the CEM cone. It should be noted that this gold film had no influence on the charging or discharging of the fracture surface on most of the materials studied due to their high resistivity.

A significant increase in FE intensity (charge released/unit area) was observed as sample cross-section was reduced. In Tables I and II, one sees that filaments a few microns in diameter were relatively intense emitters of both EE and PIE. There are two reasons most plausible for this high intensity. First, when thin filaments fracture, the freshly created fracture surface quickly becomes free of the opposite crack wall. Thus, there is less chance for the particles to hit the opposite crack wall and therefore a higher probability of reaching the CEM for detection. Secondly, filaments are known to have significantly higher tensile strengths that the bulk material, thus storing more elastic strain energy prior to fracture. This could lead to an increasing amount of excitation of the material that produces FE.

B. The Fracture of Fiber-Reinforced Epoxy

We note that single filaments and pure epoxy produce FE with a simple decay curve with time constants of a few microseconds. Figure 2 shows emission

vs time curves for the filaments as well as for pure Dow DER 332 epoxy. If we then examine the FE accompanying the fracture of fiber-reinforced epoxy strands made from the same filaments and epoxy, we find emission curves that differ considerably from the pure materials. Figures 3 and 4 show typical emission curves for a number of fiber-epoxy systems on a time scale which is very slow compared to the pure materials. First we see a rapid rise reaching a peak near the instant emission from of rupture, then a decay with a complicated time dependence. For all cases, the emission lasts far longer than for the pure materials. If we assign time constants to portions of the decay curve, they vary from ms to 5 minutes or longer. If we examine the initial portion of the curve on a faster time scale (Fig. 3b, 4b), we see events prior to catastrophic fracture of the sample, sometimes with decay constants associated with fracture of the pure samples. In Fig. 3b. the strand itself has not yet ruptured, but some filament and matrix failure has occurred. We note that the different fiber-epoxy systems presented here have different FE curves. For example, the emission from E-glass is considerably more intense and longer lasting that for S-glass. Examination under a microscope of the samples following rupture shows that there is considerably more delamination and separation of the filaments in the case of E-glass and graphite than for S-glass, S-glass showing very few clean fibers. The larger diameter E-glass filaments (20 μm compared to 10 μm) could contribute to the degree of interfacial failure.

Thus, our interpretation is as follows: Prior to rupture, the sample under tension suffers minor failures. These failures consist primarily of fiber breakage and epoxy failure and produce FE similar to that of pure materials. Finally as these minor failures accumulate, the entire strand fails, producing a large amount of delamination or interfacial failure between the filaments and epoxy. It is the latter form of failure which we believe is responsible for the major FE component with the slow decay and is possibly an

indicator of the extent of interfacial failure that has occurred. Occasionally, during the decay, smaller additional peaks in FE are observed due to further instances of minor failure because of creep of the differentially stretched materials near the broken ends of the strands. By far the predominant emission appears to be coming from the surfaces created by separation of the filaments from the matrix.

The EE from E-glass and S-glass/epoxy strands following rupture were relatively smooth curves, as were the PIE curves for all three composites. However, as seen in Fig. 3c, the EE curve from a graphite-epoxy strand is intense, but very erratic. On some samples, the emission would actually drop to zero counts for a few seconds, then jump to several thousand counts/s. Of course, one significant distinction of graphite is its high conductivity. We believe that this erratic behavior is due to surface charging and discharging that tends to alter the electron emission (but has no effect on the positive ion emission). This could occur at the interface of the graphite filament and the thin residual layer of material from the matrix.[30] Strong positive charging that occasionally discharged would explain the erratic EE and relatively smooth PIE.

E-glass/epoxy strands were also fractured in the UHV system to determine if the long lasting emission observed was due to chemi-emission from reaction of the fracture surfaces with background gases. A reduction of the background pressure by two orders of magnitude had no influence on either the EE or PIE.

When EE and PIE are compared over several samples we find that the total emission, on the average, is nearly the same. When the emission from two different samples are normalized, as shown in Fig. 5, we see that within the fluctuations of the observed particle counts, the two curves are indistinguishable. This suggests that a common rate-limiting step is occurring in EE and PIE.

By placing fine mesh grids in the regions between the sample and the CEM it is possible to make a retarding potential energy analysis[31] of the EE and PIE accompanying fracture of materials. The derivative of the count rate vs retarding grid potential is the energy distribution of the emitted particles. Figure 6 shows the results for both EE and PIE from the fracture of two different E-glass/epoxy strands. Both charges seem to have very similar energy distributions peaking near 0 eV (electron-volts), with a significant quantity of higher energy particles tailing off in the range of a few hundred eV. Although this derivative curve does not show it, approximately 15% of the particles could not be stopped by potentials in the 500-1000 volt range. The presence of these higher energy particles suggests that charging of the fracture surface (due to separation of charges) is playing a role in the ejection of these particles from the surface. The similarity of the EE and PIE energy distributions provides further support that they share a crucial mechanistic step.

A comparison of EE and PIE from the E-glass/epoxy system was made by placing an ion and electron detector on opposite sides of the sample. First, simultaneous emission of both charges was observed upon fracture. Second, the pulses coming from these detectors were tested for coincidence; i.e., within two time windows (0.5 μs and 100 μs), we asked if electrons and ions occur correlated in time. The reason for posing this question was to determine whether a portion of the elections were produced by ionization of molecules which in turn were observed as positive ions. The results were unambiguously negative. No coincidence of any statistical significance was observed in both time frames. We thus conclude that there is no evidence of simultaneous creation of electrons and ions via ionization of neutral species in the EE and PIE observed from the E-glass/epoxy system.

C. Other Long Time-Constant-Emitters

As a test of the correlation between interfacial failure and the long lasting FE, we examined a number of systems which would tend to involve failure of an adhesive-like bond. First, E-glass/epoxy strands were split lengthwise (see Fig. 7a) causing extensive delamination with only minor fiber and epoxy fracture (as determined by optical microscopy). This splitting by delamination produced the emission observed in Fig. 7a, yielding the same long time-constant emission seen in rupture of the fiber strands each time the splitting occurred (vertical arrows).

Another test involved samples of bulk epoxy bonded to glass, lucite, and aluminum in such a way that they failed in shear along the interface. The bonded area was approximately 1 cm^2. Figures 7b, c, and d show the resulting EE curves for these interfaces all exhibiting the long lasting emission.

Another type of system tested was the elastomer, polybutadiene, with and without the presence of 34% (by volume) untreated glass beads 30-95 μm in diameter. The samples were provided by The University of Akron Institute of Polymer Science. EE and PIE curves for samples with identical cross-sections are shown in Fig. 8. Although the rubber alone has relatively long lasting emission, we see that the sample containing the glass beads emits considerably stronger. Interestingly, the slow rise in emission corresponds to the relatively slow propagation of the crack in the elastomer. Gent[32] has shown that the beads become detached during straining of the material. Most likely this type of failure is responsible for the enhanced emission. The energy distribution curve for polybutadiene containing glass beads is shown in Fig. 9 and is similar to that obtained for E-glass.

Since we suspect that charge separation is involved in the release of particles when this long time-constant emission is observed, we examined a

system that is known to leave highly charged surfaces following cleavage, namely mica (muscovite). Figure 10 is the EE and PIE accompanying the fracture (cleavage) of mica, both showing the long lasting emission. Figure 11 contains the EE and PIE energy distributions from retarding potential energy analysis, and are seen to be similar to E-glass/epoxy fracture except more energetic. Although not entirely conclusive, the similarities between the mica FE and the FE from other systems suggest that charge separation may indeed be involved.

DISCUSSION

Our results show that FE is indeed a widespread phenomenon; we have not yet found a material that does not produce some form of FE. The magnitude of the emission per unit area varies considerably as does the time dependence. For all materials, the emission accompanying the motion of the crack-tip appears to be most intense. The creation of excited states would occur during this time when the energy density is the highest, and the resulting emission appears to begin immediately. (See References 4 and 6). In many materials we see a fast decay with submicrosecond time constants followed by slower decay of microseconds, milliseconds, or even many seconds. The mechanisms for the very fast vs very slow emission are likely to be quite different and need to be investigated in depth.

The results involving the fracture of epoxy-fiber systems suggest that different filament materials can alter the FE, possibly due to differences in the filament/epoxy bond and the degree of delamination that occurs. We have shown that when separation of the filament from the matrix occurs it is accompanied by a unique type of FE involving very long time constants and relatively high energy particles (a few hundred eV). Most likely, the production of such

high energy particles involves the electric fields due to charge separation that occurs when adhesive bonds are broken. Vladikina et al.[33] observe high energy electron emission from a number of systems that exhibit surface charging due to friction of dielectrics in a vacuum and by fracture. They also observe very long decay constants for friction-induced EE from polymers, an effect accompanied by intense surface charging. They attribute the observed electron emission to field emission which requires electric fields on the order of 10^6 - 10^7 V/cm and surface charge densities of 10^{-8} - 10^{-7} Coulombs/cm^2. Although it is very probable that charging is involved we are reluctant at this point to attribute the emission we observe to field emission. The main reason for this is that our energy distributions peak at or near 0 eV. One would expect the most intense EE from the highest potential points on the surface which would then produce electrons with high energy. Very low energy electrons are not likely to accompany field emission. Secondly, we find many similarities between the EE and PIE from the same type of samples, e.g. the time dependence of the emission curves and energy distributions. This suggests a common mechanism yet it is difficult to see how field emission and the production of free ions could be related.

One possible role of the electric field is the following: imagine that charge patches of varying sign and charge density are created on the surface due to separation of the crack walls. We then assume that the excitations that can produce FE, e.g., energetic defects of chemically reactive species, are able to locate in the region above the charge layer; for simplicity we would expect this to be near or at the surface of the material. Then, when de-excitation occurs, free electrons or ions are produced, and depending on the sign of the charge patch over which they are created, they may be attracted into the surface, and thereby lost, or repelled into the vacuum with kinetic

energy determined by the potential at the position where they were created. Then, the energy distributions we observed are simply a function of the distribution of charge density on the surface. The energy distribution may also be influenced by a dependence on charge density of the de-excitation probability and/or the probability of an FE-producing excitation reaching a given region. Since the charge density for good insulators has decay constants of several minutes to hours in a vacuum, the more rapid decay observed would imply that it is a measure of the supply of excited species rather than due to charge leakage. Consistent with this, we see no change in the energy distribution of either EE or PIE with time over a period of two minutes. Finally we note that the loss of charge due to leakage would be exponential, whereas the initial FE decay is much more complicated.

CONCLUSION

Considerably more work needs to be done to clearly define the various mechanisms involved for the FE observed. We are also interested in pursuing possible applications of FE to understanding fracture phenomena. For example, it is feasible that the intense emission observed during crack propagation is related to crack velocity and/or fracture mechanics parameters such as surface energy of the instantaneous stress intensity factor.

In composites or multiphase systems FE may indicate precisely where fracture is occurring, e.g. intra - vs inter-granular fracture, delamination, etc. FE may be a useful monitor of the mechano-chemistry accompanying fracture, e.g. in stress corrosion. It may also be sensitive to sub-critical crack growth. Certainly it would be an effective way to distinguish between surface cracking from internal micro-fracture in materials like ceramics since FE is a surface effect. Although still speculative at this point, it is conceivable that FE could contribute to our understanding of a wide variety of fracture phenomena.

ACKNOWLEDGMENTS

We wish to thank R. L. Moore, Lawrence Livermore Laboratory, for providing samples of filaments and fiber/epoxy strands, and Dr. A. N. Gent, University of Akron Institute of Polymer Science for supplying the polybutadiene samples. We wish to thank Dr. L. L. Clements, NASA-Ames Research Center, Dr. L. H. Peebles, Jr., and Dr. R. Miller both of Office of Naval Research, for useful discussions. We wish to acknowledge undergraduate B. J. Tillotson for his assistance in the laboratory.

REFERENCES

1. J. T. Dickinson, P. F. Bräunlich, L. Larson, and A. Marceau, Appl. Surf. Sci. 1, 515 (1978).

2. D. L. Doering, T. Oda, J. T. Dickinson, and P. F. Bräunlich, Appl. Surf. Sci. 3, 196 (1979).

3. B. Z. Rosenblum, P. F. Bräunlich, and L. Himmel, J. Appl. Phys. 48, 5262 (1977).

4. J. T. Dickinson, D. B. Snyder, and E. E. Donaldson, J. Vac. Sci. Technol. 17, 429 (1980).

5. J. T. Dickinson, D. B. Snyder, and E. E. Donaldson, Thin Solid Films,

6. J. T. Dickinson, E. E. Donaldson, and D. B. Snyder, J. Vac. Sci. Technol. 18, (1980).

7. L. A. Larson, J. T. Dickinson, P. F. Bräunlich, and D. B. Snyder, J. Vac. Sci. Technol. 16, 590 (1979).

8. A. J. Walton, Adv. Phys. 26, 887 (1977).

9. J. I. Zink, Acc. Chem. Res. 11, 289 (1978).

10. L. A. Larson, T. Oda, P. Bräunlich, and J. T. Dickinson, Solid State Comm. 32, 347 (1979).

11. K. Becker, CRC Critical Reviews in Solid State Sciences 3, 39 (1972).

12. H. Hagstrum in Experimental Methods in Catalytic Research, Vol. III, R. B. Anderson and P. T. Dawson, ed. (New York, Academic Press, 1976), pp. 42-81.

13. Yu. P. Sitonite, F. S. Zimin, T. V. Krylova, Russian J. of PHysics and Chemistry 44, 1023 (1970).

14. M. L. Knotek and P. J. Feibelman, Phys. Rev. Letters 40, 964 (1978).

15. J. Harris, B. Kasemo, and E. Tornqvist, Chem. Phys. Letters 52, 538 (1977).

16. B. Kasemo, E. Tornqvist, J. K. N. Ørskov, and B. I. Lundqvist, Surf. Sci. 89, 554 (1979).

17. G. Hoch[illegible]sser and J. F. Antonni, Surf. Sci. 32, 644 (1972).

18. E. H. [illegible]ws, "Cracking and Crazing in Polymeric Glasses," in The Physics [illegible] Glassy Polymers, R. N. Haward, ed. (New York, John Wiley and Sons, 1973), pp. 448-451.

19. M. I. Kornfeld, J. Phys. D: Appl. Phys. 11, 1295 (1978).

20. J. Wollbrandt, J. E. Linke, and K. Meyer, Phys. Stat. Sol. (A) 27, K53 (1975).

21. S. A. Hoenig, The Application of Electrostatic Techniques to the Analysis of Pre-Fracture Phenomena in Ceramic Materials, NSF Report, Contract No. ENG75-13639, August 1976.

22. B. Rosenblum, P. Braunlich, and J. P. Carrico, Appl. Phys. Letters 25, 17 (1974).

23. H. Glaefeke, in Thermally Stimulated Relaxation in Solids, P. Braunlich, ed., (Springer-Verlag, Berlin, 1979).

24. P. G. Fox and J. Soria-Ruiz, Proc. Roy. Soc. Lond. A317, 79 (1970).

25. F. Kh. Urakaev, V. V. Boldyrev, O. F. Pozdynyakov, and V. R. Regel, Kinetika i Kataliz 18, 350 (1977).

26. V. R. Regel, T. M. Muinov, and O. F. Pozdynyakov, in Physical Basis of Yield and Fracture, (Institute of Physics, London, 1966), p. 194.

27. J. R. Asay, "A Model for Estimating the Effects of Surface Roughness on Mass Ejection from Shocked Materials," Sandia Laboratories Report SAND78-1256 (1978).

28. B. Hayes, private communication.

29. E. A. Kurz, American Laboratory, March 1979, p.67.

30. L. H. Sharpe, J. Adhesion 4, 51 (1972).

31. J.H.D. Eland, Photoelectron Spectroscopy, (Butterworths, London, 1974), pp 34-37.

32. A. N. Gent, private communication.

33. T. N. Vladikina, B. V. Derjaguin, V. A. Kluev, Yu. P. Toporov, and Yu. A. Khrustalev, Transactions of the ASME, 102, 552 (1980).

TABLE I

ELECTRONS

MATERIALS	APPROX. DECAY TIMES OF FRACTO-EMISSION	ELECTRONS DETECTED/ cm^2 OF CRACK WALL
Sapphire	<1 s, minutes	10^3
Alumina	<1 s, minutes	10^4
Al_2O_3 Anodized Layer	.1 - 20 μsec	10^5
BN	<1 s, minutes	10^6
Quartz	<1 s, minutes	10^6
Mica (Muscovite)	1 s, minutes	10^6
Crystalline Sugar	<1 s, minutes	10^6
Fused Silica	Several ms	10^3
Soda Lime Glass	Several ms	10^3
Kelvar 49 Fibers	<<.1 s	10^8
Graphite Fibers	10 μs	10^8
E Glass Fibers	10 μs	10^8
S Glass Fibers	10 μs	10^8
Epoxy (DER 332)	25 μs	10^3
Lucite	<2 ms	10^2
Polystyrene	500 μs, 12.3 μs	10^3
ELASTOMERS		
Neoprene	<1 s	10^2
Viton	<1 s	10^3
Buna N	<1 s	10^2
Natural Rubber	<1 s	10^3
Natural Rubber (abraded)	minutes	10^7
Silicone Rubber	<1 s, minutes	10^5
Solathane	<.2 s	10^4
Vinyl Rubber-filled	<1 s, minutes	10^4
Polybutadiene	0.04 s, minutes	10^3
Polybutadiene-filled	<1 s, minutes	10^7

TABLE II

POSITIVE IONS

MATERIAL	APPROX. DECAY TIMES OF FRACTO-EMISSION	IONS DETECTED cm^2 OF CRACK WALL
Mica (Muscovite)	1 s, minutes	10^6
FIBERS		
Kevlar 49	<0.1 s	10^8
Carbon	10 μs	10^8
E-glass	10 μs	10^7
S-glass	11 μs	10^8
PLASTICS		
Epoxy (DER 332)	25 μs	10^3
Lucite	<2 msec	10^2
Polystyrene	35 μs	10^4
ELASTOMERS		
Buna N	<1 s, minutes	10^3
Natural Rubber	<1 s	10^4
Natural Rubber (abraded)	minutes	10^7
Silicone Rubber	<1 s, minutes	10^3
Solathane	<.1 s	10^6
Vinyl Rubber-filled	<1 s, minutes	10^5
Polybutadiene	<.04 s, minutes	10^5
Polybutadiene-filled	<.2 s, minutes	10^6

FIGURE CAPTIONS

1. The time distributions of electron emission due to the fracture of

   (a) polystrene. (b) boron nitride.

2. The time distributions of electron emission due to the fracture of graphite and glass filaments (10 μm in diameter) and bulk epoxy (Dow DER 332). Note the fast time scale.

3. Electron emission during and following fracture of fiber/epoxy strands. Note the range of time scales.

4. Positive ion emission accompanying and following fracture of fiber/epoxy strands.

5. Comparison of electron emission and positive ion emission due to fracture of E-glass/epoxy strands. The PIE data has been normalized to the EE data.

6. Energy distributions of electrons and ions from fracture of E-glass/epoxy strands. Obtained by differentiation of retarding potential analysis of the emitted particles.

7. Electron emission during and following interfacial failure between epoxy and other materials: (a) split E-glass/epoxy strands (b) sode-lime glass (c) lucite (d) aluminum

8. The emission curves for electrons and positive ions from the fracture of polybutadiene filled and unfilled with small glass beads.

9. The energy distribution of electrons produced by fracture of polybutadiene containing glass beads.

10. Fracto-emission curves for mica showing time dependence of both electrons and positive ions.

11. Energy distributions of electrons and positive ions arising from the fracture of mica.

(a)

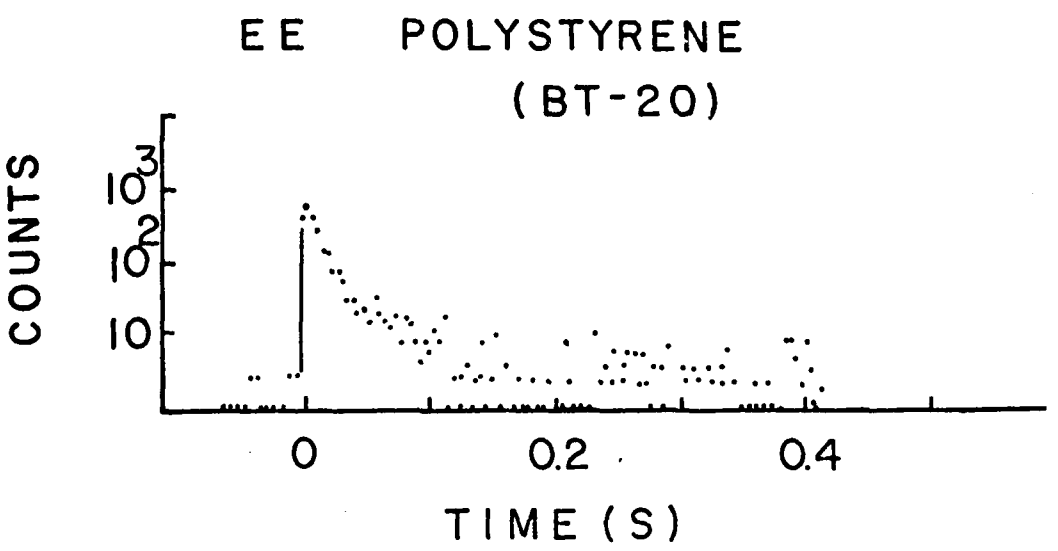
EE POLYSTYRENE
(BT-20)
COUNTS
10³
10²
10
0
0.2
0.4
TIME (S)

(b)

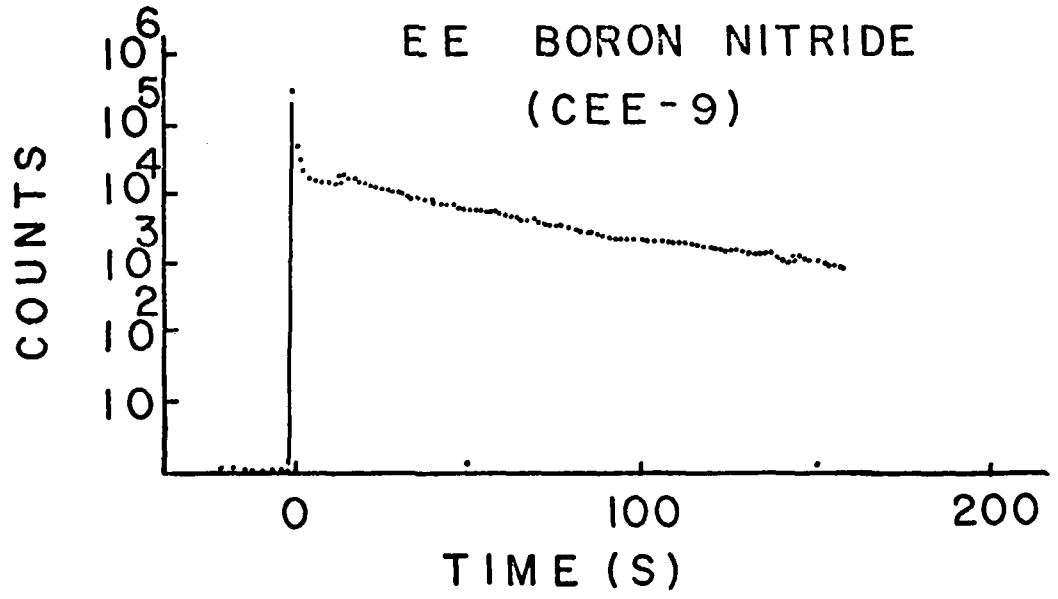
EE BORON NITRIDE
(CEE-9)
COUNTS
10⁶
10⁵
10⁴
10³
10²
10
0
100
200
TIME (S)

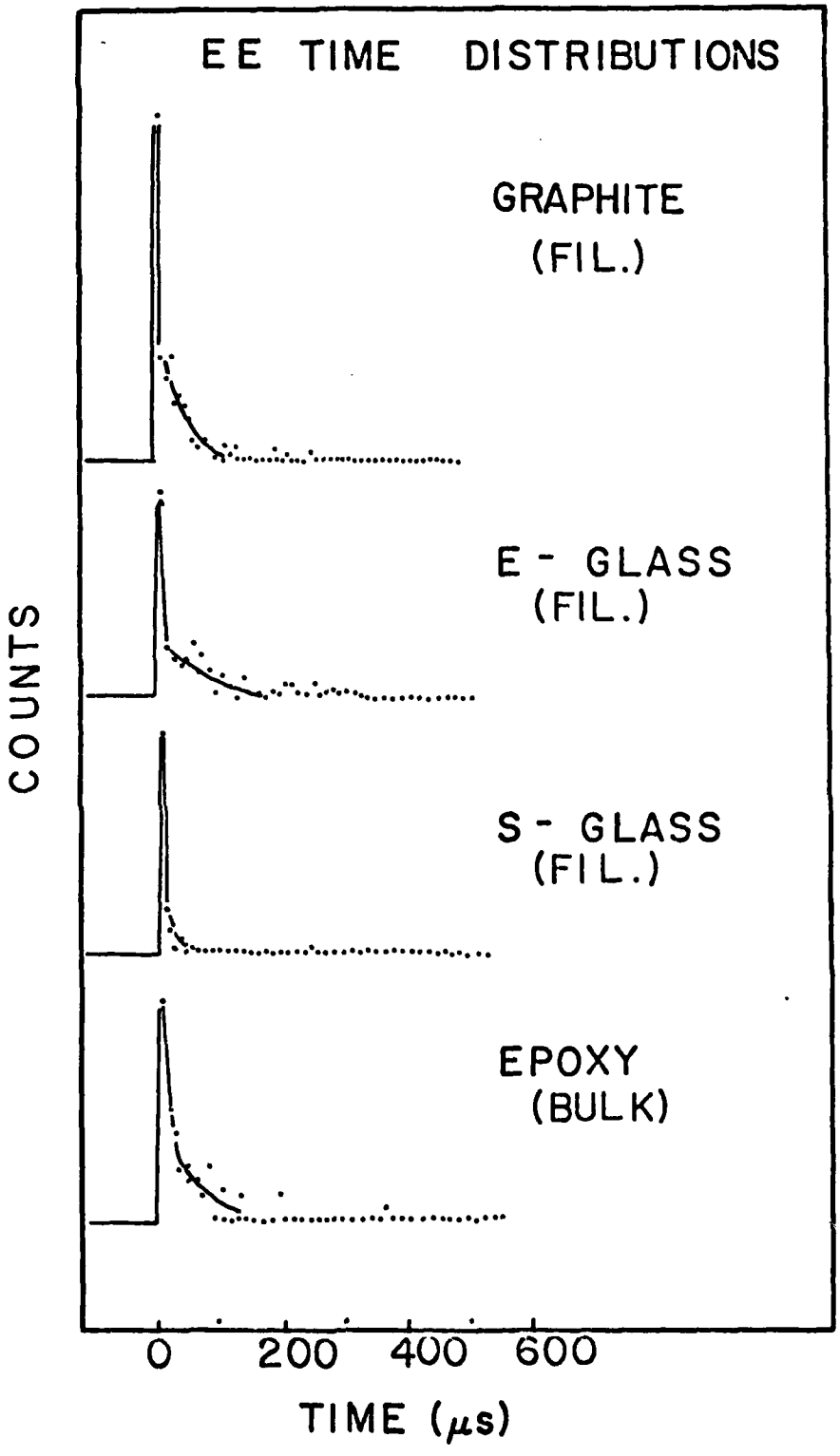
EE TIME DISTRIBUTIONS
GRAPHITE
(FIL.)
E - GLASS
(FIL.)
S - GLASS
(FIL.)
EPOXY
(BULK)
COUNTS
0
200
400
600
TIME (μs)

ELECTRON EMISSION FROM FRACTURE OF FIBER - REINFORCED EPOXY UNDER TENSILE STRAIN

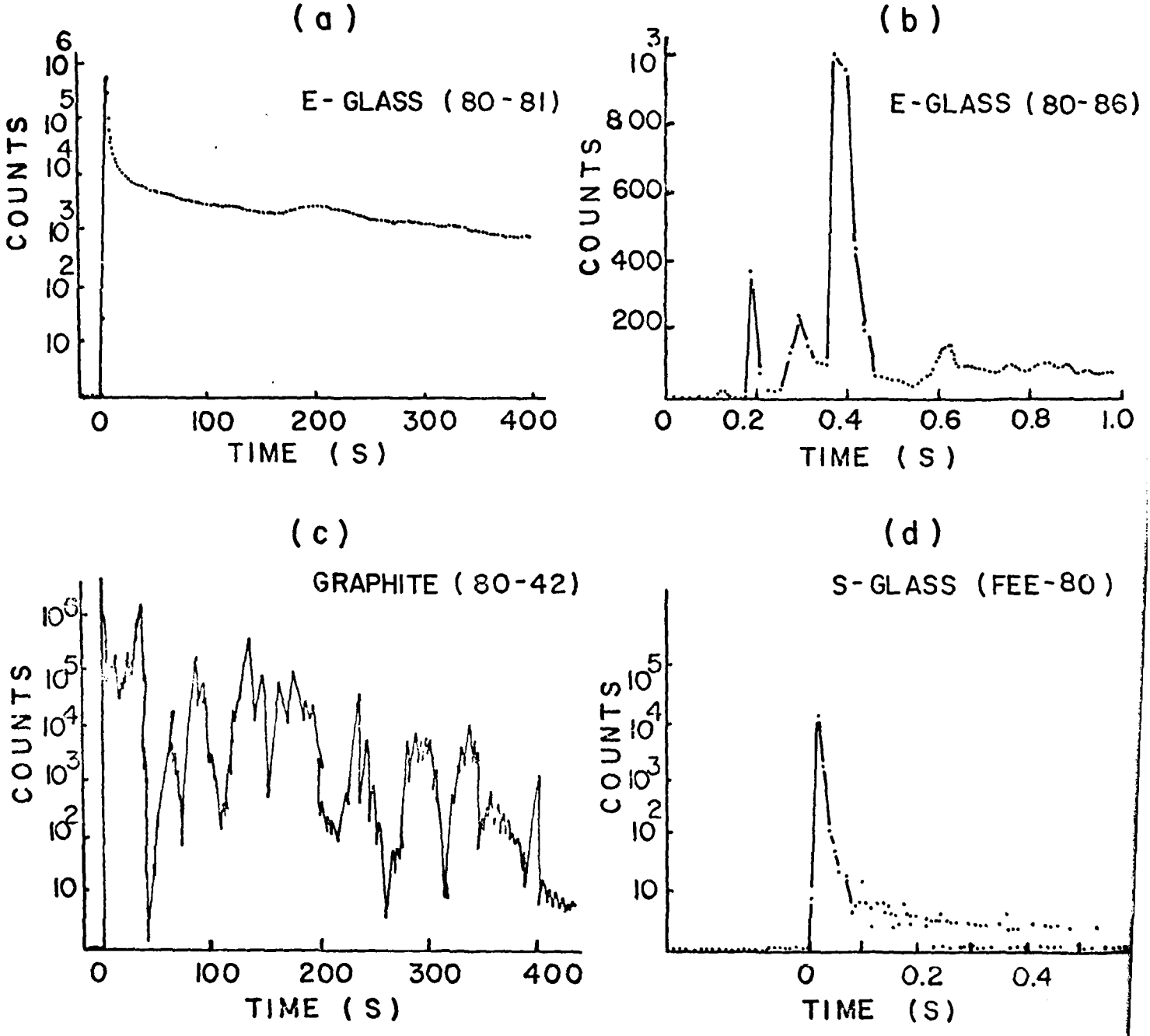

POSITIVE ION EMISSION

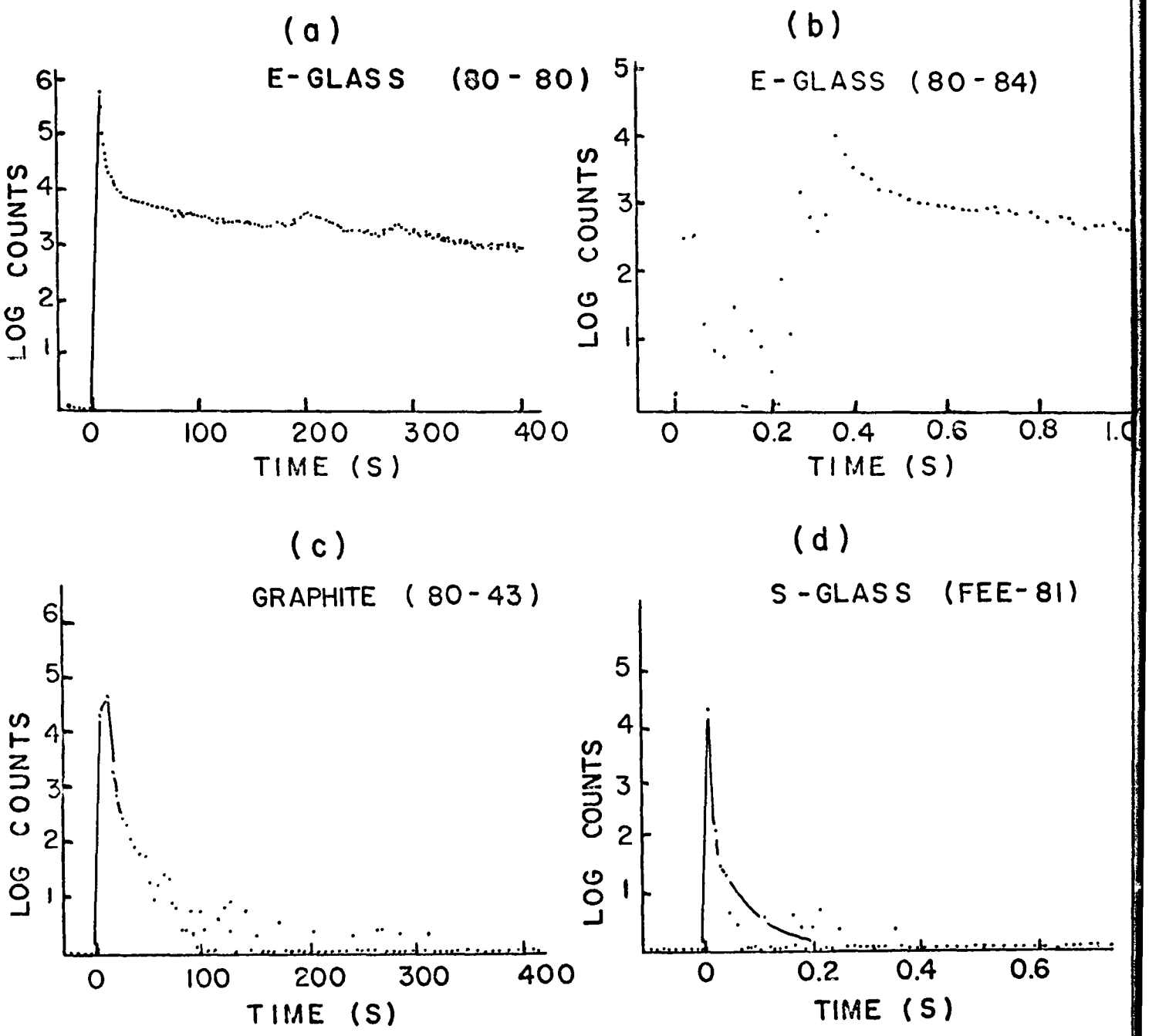

COMPARISON OF EE AND PIE FROM E-GLASS/EPOXY STRANDS

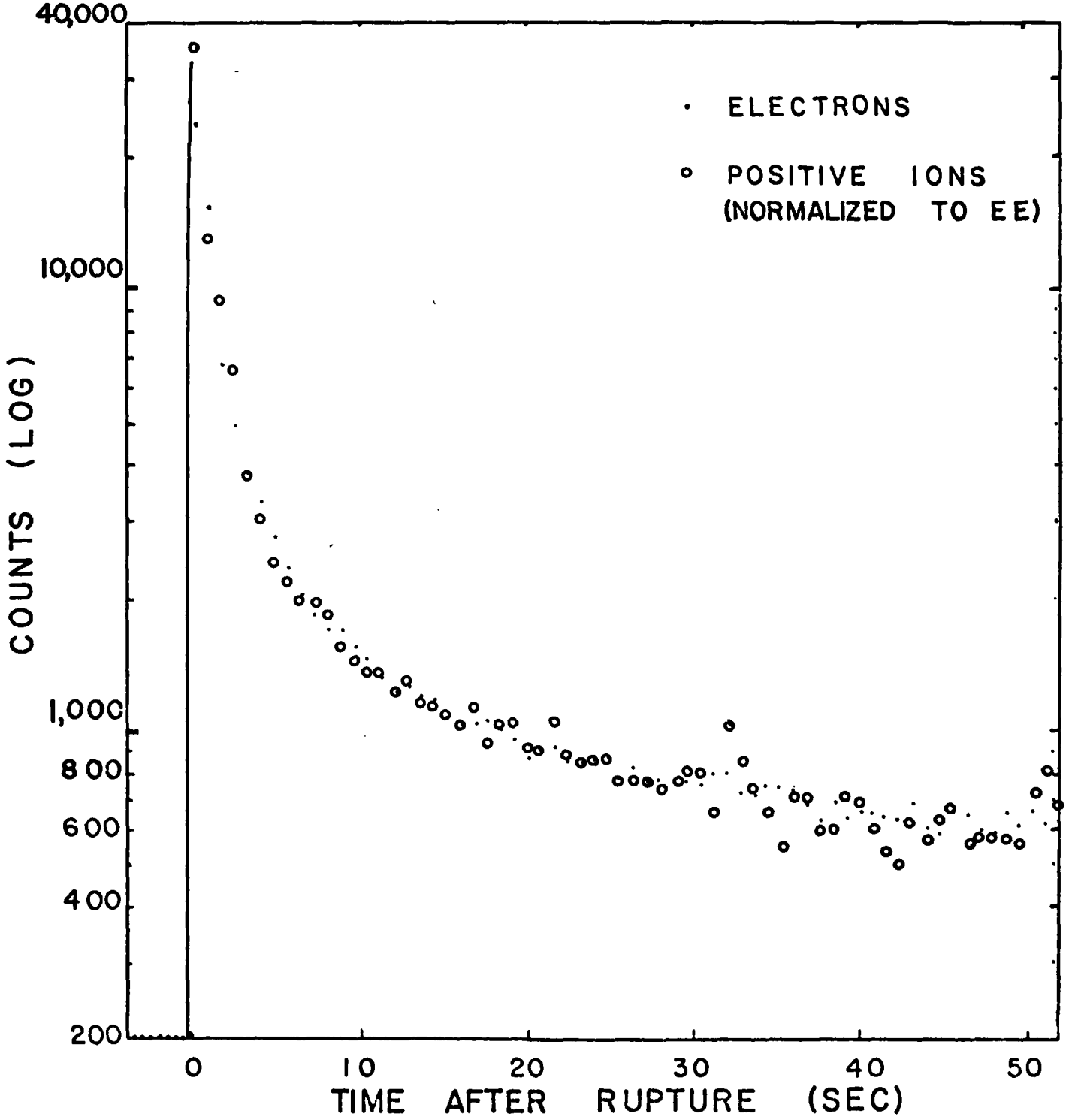

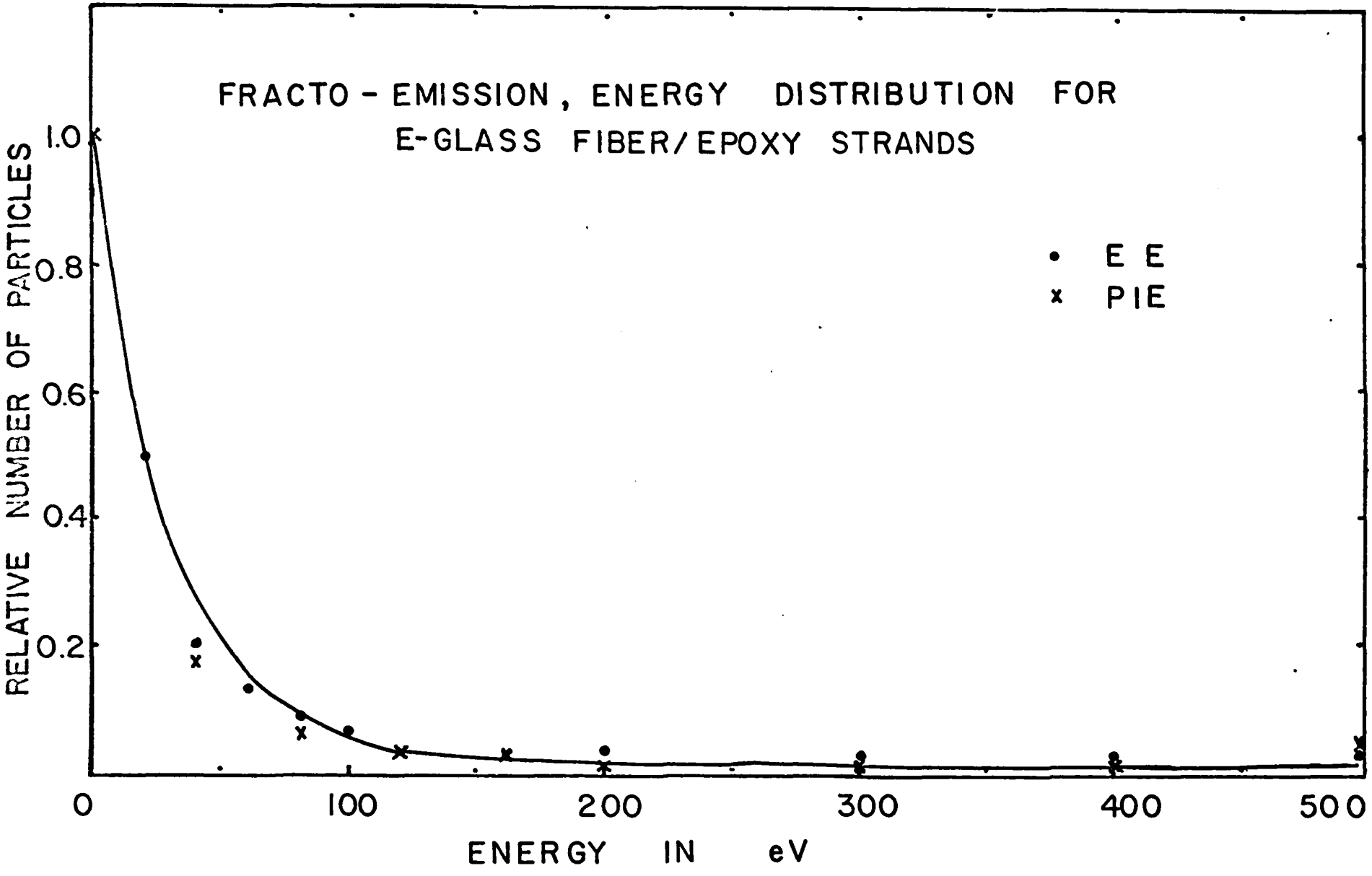
FRACTO - EMISSION, ENERGY DISTRIBUTION FOR
E-GLASS FIBER/EPOXY STRANDS
E E
PIE
RELATIVE NUMBER OF PARTICLES
1.0
0.8
0.6
0.4
0.2
0
100
200
300
400
500
ENERGY IN eV

ELECTRON EMISSION

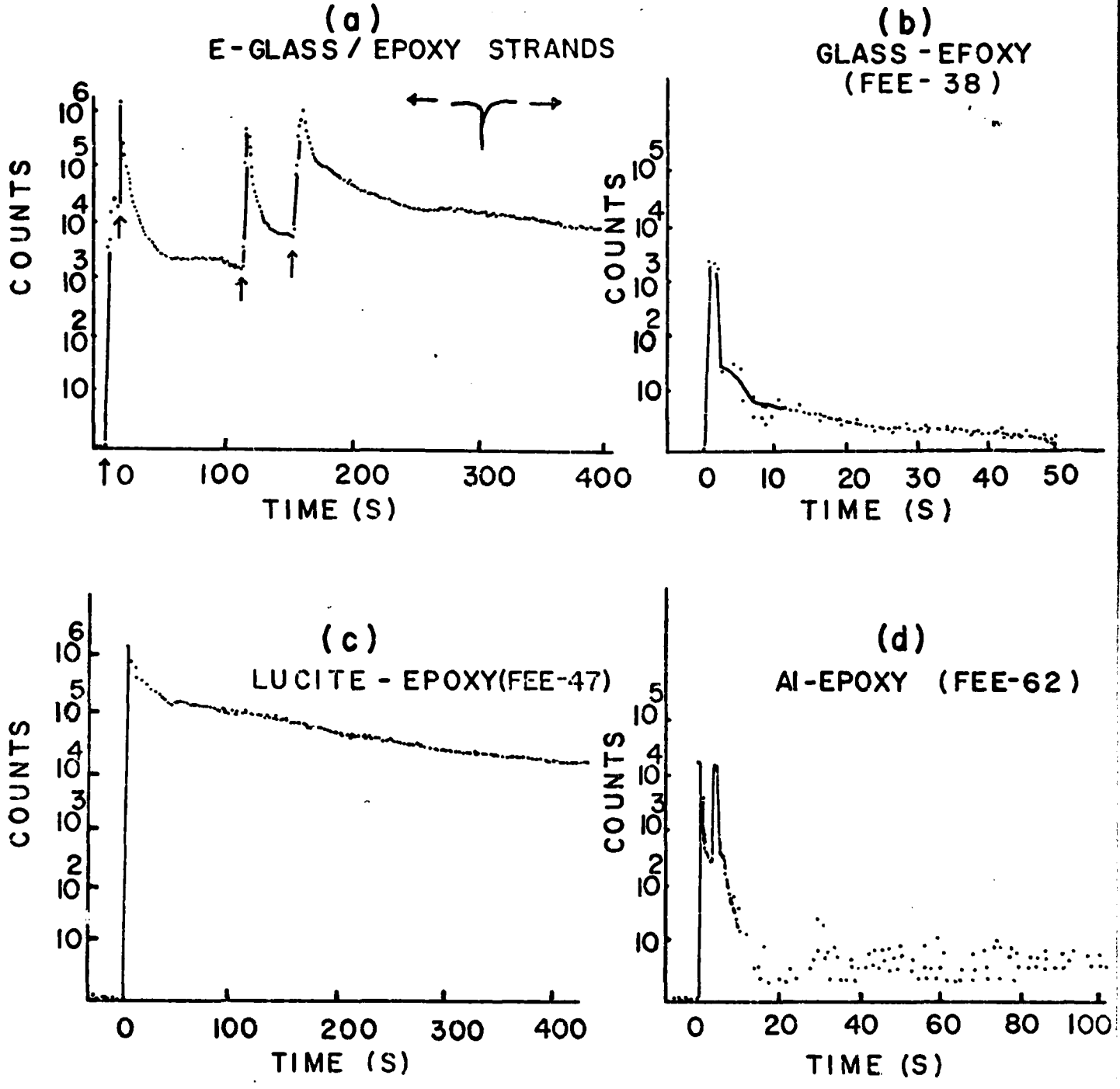

POLYBUTADIENE

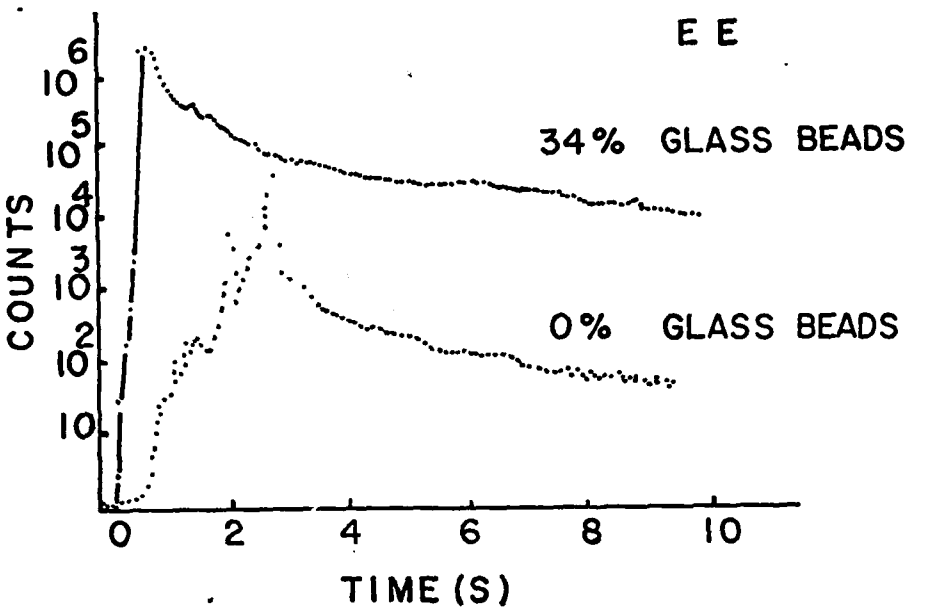

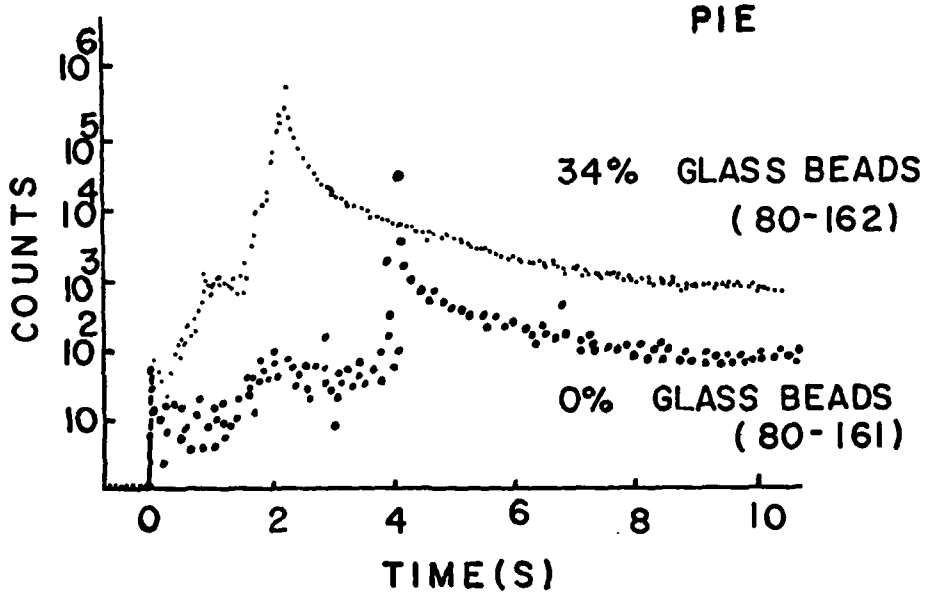

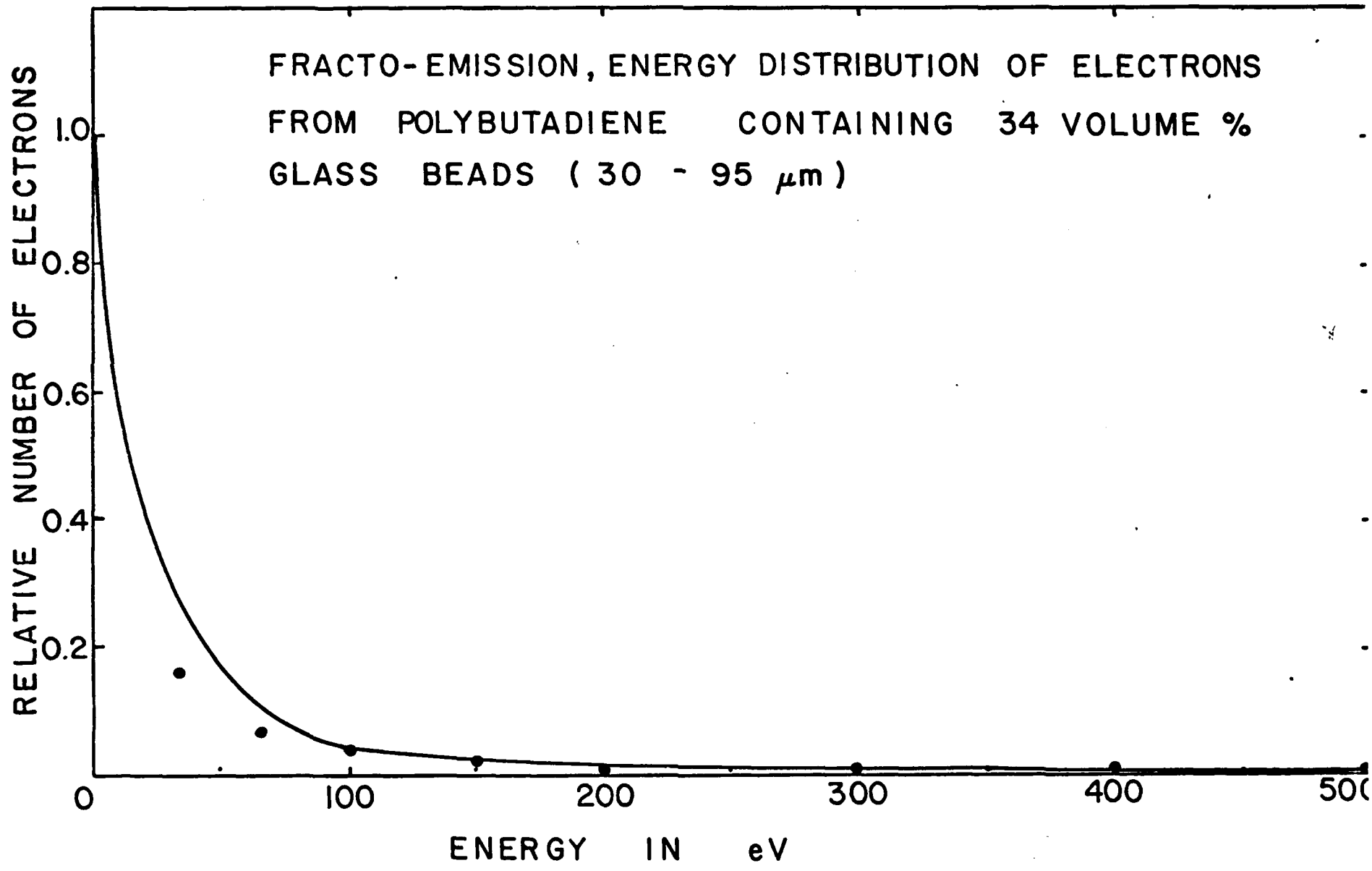
FRACTO-EMISSION, ENERGY DISTRIBUTION OF ELECTRONS
FROM POLYBUTADIENE CONTAINING 34 VOLUME %
GLASS BEADS (30 - 95 μm)
RELATIVE NUMBER OF ELECTRONS
1.0
0.8
0.6
0.4
0.2
0
100
200
300
400
500
ENERGY IN eV

Fig. 1

FRACTO - EMISSION FROM MICA

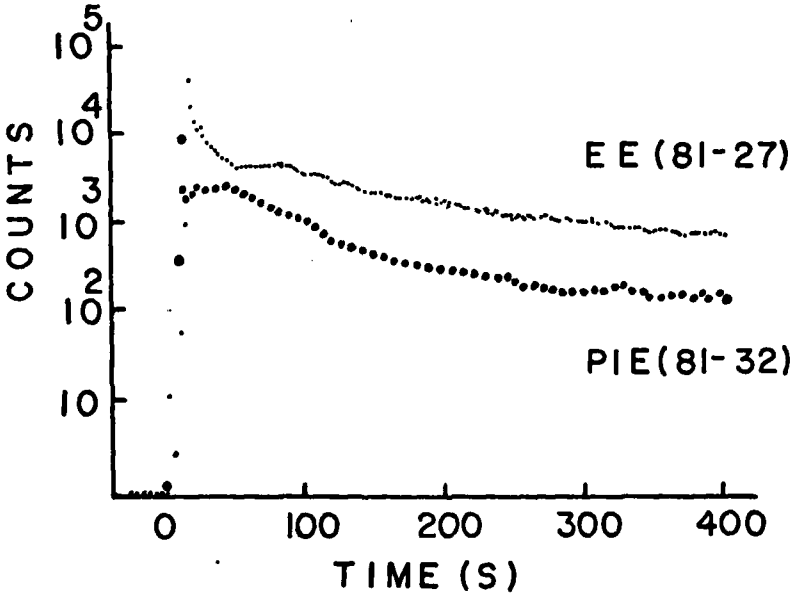

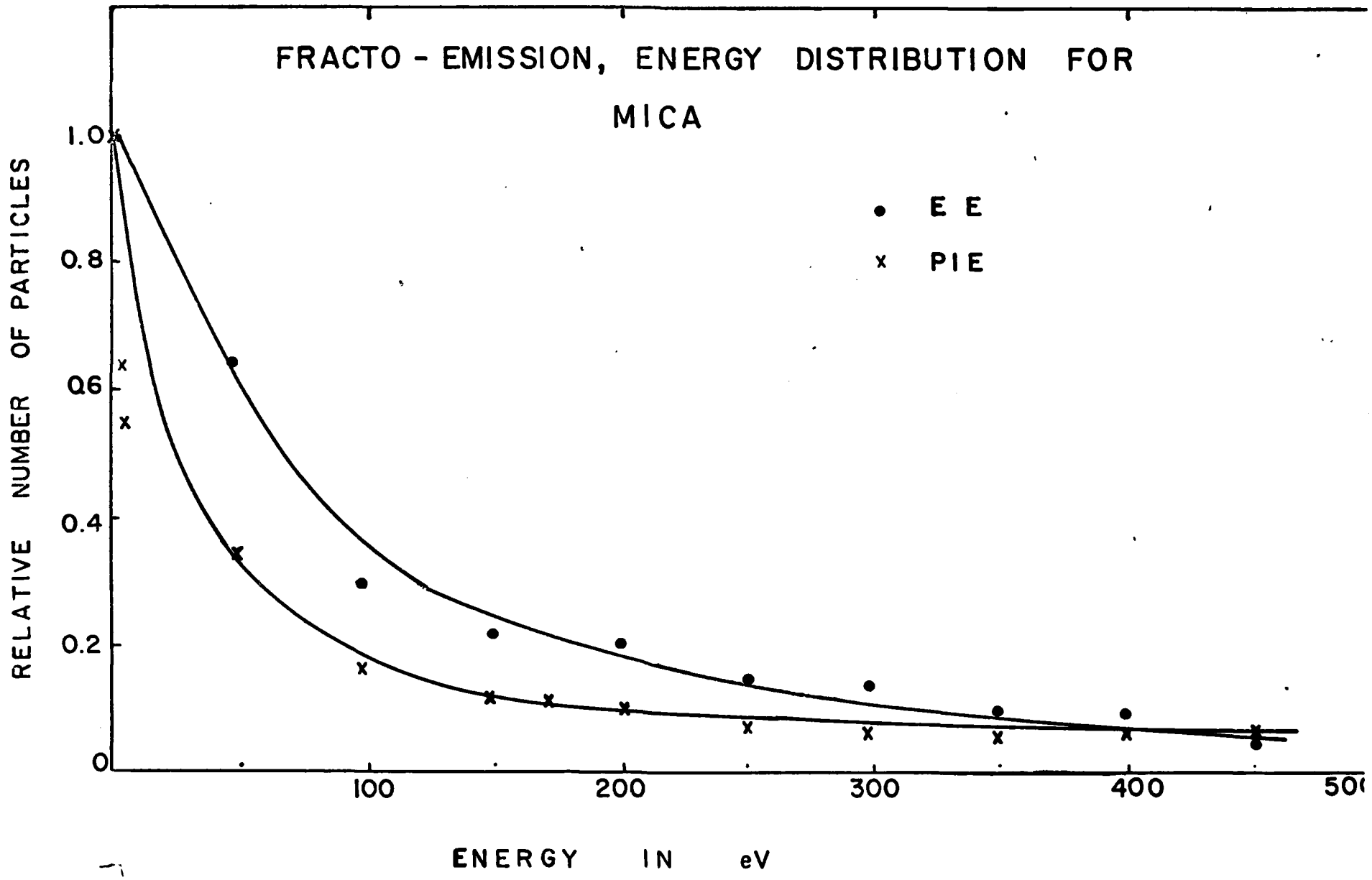
FRACTO - EMISSION, ENERGY DISTRIBUTION FOR MICA
E E
PIE
RELATIVE NUMBER OF PARTICLES
1.0
0.8
0.6
0.4
0.2
0
100
200
300
400
ENERGY IN eV

DEF.

ENERGETIC MATERIALS RESEARCH

DISTRIBUTION LIST

	No. Copies
Assistant Secretary of the Navy (R, E, and S) Attn: Dr. R.E. Reichenbach Room 5E787 Pentagon Washington, DC 20350	1
Office of Naval Research Code 473 Arlington, VA 22217 Attn: Dr. R. Miller	10
Office of Naval Research Code 200B Arlington, VA 22217 Attn: Dr. J. Enig	1
Office of Naval Research Code 260 Arlingon, VA 22217 Attn: Mr. D. Siegel	1
Office of Naval Research Western Office 1030 East Green Street Pasadena, CA 91106 Attn: Dr. T. Hall	1
Office of Naval Research Eastern Central Regional Office 495 Summer Street Boston, MA 02210 Attn: Dr. L. Peebles Dr. A. Wood	2
Office of Naval Research San Francisco Area Office One Hallidie Plaza Suite 601 San Francisco, CA 94102 Attn: Dr. P. A. Miller	1
Defense Technical Information Center DTIC-DDA-2 Cameron Station Alexandria, VA 22314	12
AFATL Eglin AFB, FL 32542 Attn: Dr. Otto K. Heiney	1
AFRPL Code PACC Edwards AFB, CA 93523 Attn: Mr. W. C. Andrepont	1
AFRPL Code CA Edwards AFB, CA 93523 Attn: Dr. R. R. Weiss	1
Code AFRPL MKPA Edwards AFB, CA 93523 Attn: Mr. R. Geisler	1
Code AFRPL MKPA Edwards AFB, CA 93523 Attn: Dr. F. Roberto	1
AFSC Andrews AFB, Code DLFP Washington, DC 20334 Attn: Mr. Richard Smith	1
Air Force Office of Scientific Research Directorate of Chemical & Atmospheric Sciences Bolling Air Force Base Washington, DC 20332	1
Air Force Office of Scientific Research Directorate of Aerospace Sciences Bolling Air Force Base Washington, DC 20332 Attn: Dr. L. H. Caveny	1
Anal-Syn Lab Inc. P.O. Box 547 Paoli, PA 19301 Attn: Dr. V. J. Keenan	1

DEF.

	No. Copies
Army Ballistic Research Labs Code DRDAR-BLP Aberdeen Proving Ground, MD 21005 Attn: Mr. L. A. Watermeier	1
Army Ballistic Research Labs ARRADCOM Code DRDAR-BLP Aberdeen Proving Ground, MD 21005 Attn: Dr. Ingo W. May	1
Army Ballistic Research Labs ARRADCOM Code DRDAR-BLT Aberdeen Proving Ground, MD 21005 Attn: Dr. Philip Howe	1
Army Missile Command Code DRSME-RK Redstone Arsenal, AL 35809 Attn: Dr. R. G. Rhoades Dr. W. W. Wharton	2
Atlantic Research Corp. 5390 Cherokee Avenue Alexandria, VA 22314 Attn: Dr. C. B. Henderson	1
Ballistic Missile Defense Advanced Technology Center P.O. Box 1500 Huntsville, AL 35807 Attn: Dr. David C. Sayles	1
Ballistic Research Laboratory USA ARRADCOM DRDAR-BLP Aberdeen Proving Ground, MD 21005 Attn: Dr. A. W. Barrows	1
Hercules Inc. Cumberland Aerospace Division Allegany Ballistics Lab P.O. Box 210 Cumberland, MD 21502 Attn: Dr. Rocco Musso	2
Hercules Inc. Eglin AFATL/DLDL Eglin AFB, FL 32542 Attn: Dr. Ronald L. Simmons	1
Hercules Inc. Magna Bacchus Works P.O. Box 98 Magna, UT 84044 Attn: Mr. E. H. DeButts	1
Hercules Inc. Magna Bacchus Works P.O. Box 98 Magna, UT 84044 Attn: Dr. James H. Thacher	1
HQ US Army Material Development Readiness Command Code DRCDE-DW 5011 Eisenhower Avenue Room 8N42 Alexandria, VA 22333 Attn: Mr. S. R. Matos	1
Johns Hopkins University APL Chemical Propulsion Information Agency Johns Hopkins Road Laurel, MD 20810 Attn: Mr Theodore M. Gilliland	1
Lawrence Livermore Laboratory University of California Livermore, CA 94550 Attn: Dr. M. Finger	1
Lawrence Livermore Laboratory University of California Livermore, CA 94550 Attn: Dr. R. McGuire	1
Lockheed Missiles and Space Co. P.O. Box 504 Sunnyvale, CA 94088 Attn: Dr. Jack Linsk Org. 83-10 Bldg. 154	1

DEF.

	No. Copies
Lockheed Missile & Space Co. 3251 Hanover Street Palo Alto, CA 94304 Attn: Dr. H. P. Marshall Dept. 52-35	1
Los Alamos Scientific Lab P.O. Box 1663 Los Alamos, NM 87545 Attn: Dr. R. Rogers, WX-2	1
Los Alamos Scientific Lab P.O. Box 1663 Los Alamos, NM 87545 Attn: Dr. B. Craig, M Division	1
Naval Air Systems Command Code 330 Washington, DC 20360 Attn: Mr. R. Heitkotter Mr. R. Brown	1
Naval Air Systems Command Code 310 Washington, DC 20360 Attn: Dr. H. Mueller Dr. H. Rosenwasser	1
Naval Explosive Ordnance Disposal Facility Indian Head, MD 20640 Attn: Lionel Dickinson Code D	1
Naval Ordnance Station Code 5034 Indian Head, MD 20640 Attn: Mr. S. Mitchell	1
Naval Ordnance Station Code PM4 Indian Head, MD 20640 Attn: Mr. C. L. Adams	1
Dean of Research Naval Postgraduate School Monterey, CA 93940 Attn: Dr. William Tolles	1
Naval Research Lab Code 6510 Washington, DC 20375 Attn: Dr. J. Schnur	1
Naval Research Lab Code 6100 Washington, DC 20375	1
Naval Sea Systems Command Washington, DC 20362 Attn: Mr. G. Edwards, Code 62R3 Mr. J. Murrin, Code 62R2 Mr. W. Blaine, Code 62R	1
Naval Sea Systems Command Washington, DC 20362 Attn: Mr. R. Beauregard SEA 64E	1
Naval Surface Weapons Center Code R11 White Oak, Silver Spring, MD 20910 Attn: Dr. H. G. Adolph	1
Naval Surface Weapons Center Code R13 White Oak, Silver Spring, MD 20910 Attn: Dr. R. Bernecker	1
Naval Surface Weapons Center Code R10 White Oak, Silver Spring, MD 20910 Attn: Dr. S. J. Jacobs	1
Naval Surface Weapons Center Code R11 White Oak, Silver Spring, MD 20910 Attn: Dr. M. J. Kamlet	1
Naval Surface Weapons Center Code R04 White Oak, Silver Spring, MD 20910 Attn: Dr. D. J. Pastine	1
Naval Surface Weapons Center Code R13 White Oak, Silver Spring, MD 20910 Attn: Dr. E. Zimet	1

DEF.

	No. Copies
Naval Surface Weapons Center Code R101 Indian Head, MD 20640 Attn: Mr. G. L. MacKenzie	1
Naval Surface Weapons Center Code R17 Indian Head, MD 20640 Attn: Dr. H. Haiss	1
Naval Surface Weapons Center Code R11 White Oak, Silver Spring, MD 20910 Attn: Dr. K. F. Mueller	1
Naval Surface Weapons Center Code R16 Indian Head, MD 20640 Attn: Dr. T. D. Austin	1
Naval Surface Weapons Center Code R122 White Oak, Silver Spring, MD 20910 Attn: Mr. L. Roslund	1
Naval Surface Weapons Center Code R121 White Oak, Silver Spring, MD 20910 Attn: Mr. M. Stosz	1
Naval Weapons Center Code 3853 China Lake, CA 93555 Attn: Dr. R. Atkins	1
Naval Weapons Center Code 3205 China Lake, CA 93555 Attn: Dr. L. Smith	1
Naval Weapons Center Code 3205 China Lake, CA 93555 Attn: Dr. C. Thelen	1
Naval Weapons Center Code 385 China Lake, CA 93555 Attn: Dr. A. Amster	1
Naval Weapons Center Code 388 China Lake, CA 93555 Attn: D. R. Derr	1
Naval Weapons Center Code 388 China Lake, CA 93555 Attn: Dr. R. Reed Jr.	1
Naval Weapons Center Code 385 China Lake, CA 93555 Attn: Dr. A. Nielsen	1
Naval Weapons Center Code 3858 China Lake, CA 93555 Attn: Mr. E. Martin	1
Naval Weapons Center China Lake, CA 93555 Attn: Mr. R. McCarten	1
Naval Weapons Support Center Code 5042 Crane, Indiana 47522 Attn: Dr. B. Douda	1
Rohm and Haas Company 723-A Arcadia Circle Hunsville, Alabama 35801 Attn: Dr. H. Shuey	1
Strategic Systems Project Office Dept. of the Navy Room 901 Washington, DC 20376 Attn: Dr. J. F. Kincaid	1
Strategic Systems Project Office Dept. of the Navy Room 1048 Washington, DC 20376 Attn: Mr. E. L. Throckmorton Mr. R. Kinert	2
Thiokol Chemical Corp. Brigham City Wasatch Division Brigham City, UT 84302 Attn: Dr. G. Thompson	1

DEF.

	No. Copies
USA ARRADCOM DRDAR-LCE Dover, NJ 07801 Attn: Dr. R. F. Walker	1
USA ARRADCOM DRDAR-LCE Dover, NJ 07801 Attn: Dr. N. Slagg	1
U.S. Army Research Office Chemistry Division P.O. Box 12211 Research Triangle Park, NC 27709	1
Institute of Polymer Science University of Akron Akron, OH 44325 Attn: Professor Alan N. Gent	1
SRI International 333 Ravenswood Avenue Menlo Park, CA 94025 Attn: Dr. Y.M. Gupta	1
Graduate Aeronautical Lab. California Institute of Technology Pasadena, CA 91125 Attn: Professor W.G. Knauss	1
Pennsylvania State University Dept. of Mechanical Engineering University Park, PA 16802 Attn: Professor Kenneth Kuo	1
Office of Naval Research 800 N. Quincy St. Arlington, VA 22217 Attn: Dr. G. Neece Code 472	1
Thiokol Corp. Huntsville Huntsville Div. Huntsville, AL 35807 Attn: Mr. J.D. Byrd	1
Washington State University- Dept. of Physics Pullman, WA 99163 Attn: Prof. T. Dickinson	1
University of California Dept. of Chemistry 405 Hilgard Avenue Los Angeles, CA 90024 Attn: Prof. M.F. Nicol	1
Georgia Institute of Technology Office of Research Administration Atlanta, Georgia 30332 Attn: Professor Edward Price	1
Univ. of Utah Dept. of Mech. & Industrial Engineering MEB 3008 Salt Lake City, Utah 84112 Attn: Dr. Stephen Swanson	1
Space Sciences, Inc. 135 Maple Avenue Monrovia, CA 91016 Attn: Dr. M. Farber	1
Washington State University Dept. of Physics Pullman, WA 99163 Attn: Professor G.D. Duvall	1
Univ. of Maryland Department of Mechanical Eng. College Park, MD 20742 Attn: Professor R.W. Armstrong	1
The Catholic University of America Physics Department 520 Michigan Ave., N.E. Washington, D.C. 20017 Attn: Professor T. Litovitz	1
Sandia Laboratories Division 2513 P.O. Box 5800 Albuquerque, N.M. 87185 Attn: Dr. S. Sheffield	1
IBM Research Lab. K42.282 San Jose, CA 95193 Attn: Dr. Thor L. Smith	1
California Institute of Tech. Dept. of Chemical Engineering Pasadena, CA 91125 Attn: Professor N.W. Tschoegl	1
Northwestern University Dept. of Civil Engineering Evanston, IL 60201 Attn: Professor J.D. Achenbach	1
Office of Naval Research Structural Mechanics Program Arlington, VA 22217 Attn: Dr. N.L. Basdekas, Code 474	1

DEF.

	No. Copies
University of California Berkeley, CA 94720 Attn: Prof. A.G. Evans	1
Texas A&M Univ. Dept. of Civil Engineering College Station, TX 77843 Attn: Professor Richard A. Schapery	1
SRI International 333 Ravenswood Ave. Menlo Park, CA 94025 Attn: Mr. M. Hill	1
Los Alamos Scientific Laboratory Los Alamos, NM 87545 Attn: Dr. J.M. Walsh	1

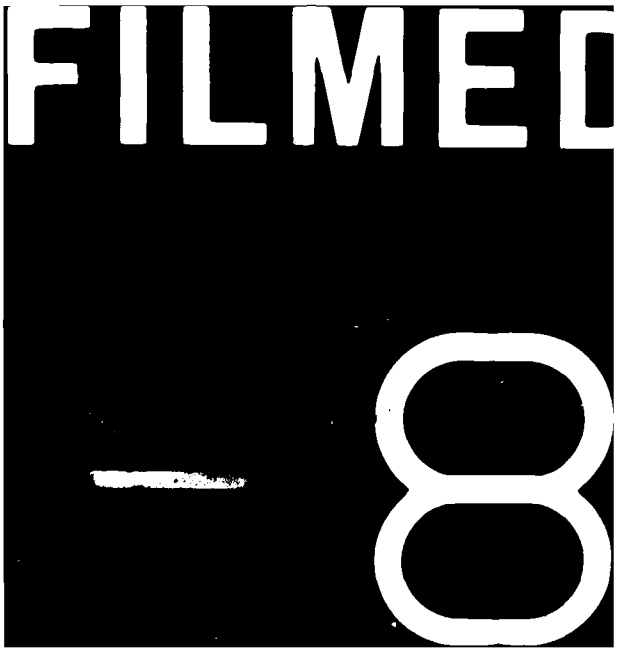
FILME
8